Biochimica et Biophysica Acta 1798 (2010) 210–215

Contents lists available at ScienceDirect

Biochimica et Biophysica Acta

journal homepage: www.elsevier.com/locate/bbamem

Solid-state ^{2}H and ^{15}N NMR studies of side-chain and backbone dynamics of phospholamban in lipid bilayers: Investigation of the N27A mutation

Shidong Chu, Aaron T. Coey, Gary A. Lorigan *

Department of Chemistry and Biochemistry, Miami University, Oxford, OH 45056, USA

ARTICLE INFO

Article history:
Received 20 April 2009
Received in revised form 18 September 2009
Accepted 30 September 2009
Available online 17 October 2009

Keywords:
Phospholamban
Phospholipid membrane
Solid-state NMR
Dynamics

ABSTRACT

Phospholamban (PLB) is an integral membrane protein regulating Ca^{2+} transport through inhibitory interaction with sarco(endo)plasmic reticulum calcium ATPase (SERCA). The Asn27 to Ala (N27A) mutation of PLB has been shown to function as a superinhibitor of the affinity of SERCA for Ca^{2+} and of cardiac contractility *in vivo*. The effects of this N27A mutation on the side-chain and backbone dynamics of PLB were investigated with ^{2}H and ^{15}N solid-state NMR spectroscopy in phospholipid multilamellar vesicles (MLVs). ^{2}H and ^{15}N NMR spectra indicate that the N27A mutation does not significantly change the side-chain or backbone dynamics of the transmembrane and cytoplasmic domains when compared to wild-type PLB. However, dynamic changes are observed for the hinge region, in which greater mobility is observed for the CD_3-labeled Ala24 N27A-PLB. The increased dynamics in the hinge region of PLB upon N27A mutation may allow the cytoplasmic helix to more easily interact with the Ca^{2+}-ATPase; thus, showing increased inhibition of Ca^{2+}-ATPase.

1. Introduction

Phospholamban (PLB) is a 52-amino acid integral membrane protein that regulates the activity of sarco(endo)plasmic reticulum calcium ATPase (SERCA), which controls the uptake of Ca^{2+} from the sarcoplasmic reticulum (SR). This mechanism controls the contraction–relaxation cycle of the heart [1,2]. The relief of SERCA inhibition is achieved by phosphorylation of PLB at Ser16 by protein kinase A and/or Thr17 by Ca^{2+}/calmodulin-dependent protein kinases [3]. In its non-phosphorylated form, PLB inhibits SERCA activity, whereas phosphorylation of PLB relieves the inhibition. PLB also oligomerizes into pentamers through a leucine–isoleucine zipper interaction in the transmembrane domain [4]. Several studies revealed that the PLB pentamer depolymerizes into active monomers that bind and inhibit SERCA and that an L37A mutation destabilizes the PLB oligomers [4–6]. Recent studies have also indicated that the pentameric form of PLB can co-crystallize with SERCA [7].

Solution NMR, solid-state NMR, and EPR spectroscopic techniques have been extensively used to investigate the structure and dynamics of membrane proteins in general and PLB in particular in various membrane environments [8–18]. In dodecylphosphocholine (DPC) micelles, monomeric AFA-PLB (where all three native Cys residues 36, 41 and 46 of PLB are replaced with Ala) takes on an "L-shape" with a cytoplasmic a-helical domain Ia (residues 2–16) connected to another transmembrane a-helical domain (residues 22–50) through a loop (residues17–21) [12] (Fig. 1). Based on nuclear spin relaxation and solvent accessibility experiments, the segment 23–52 is further subdivided into two dynamic domains: domain Ib (residues 23–30) and domain II (residues 31–52) [14]. One of the noticeable diversities in the reported structures of PLB, however, is the structure and dynamics of the cytoplasmic domain. In the "pinwheel" structure of the wild-type pentameric form of PLB, the cytoplasmic domains interact with the membrane surface, and a dynamic equilibrium between the two conformational states ("L-shaped" form or "T-state", and extended form or "R state") was proposed to account for the regulatory mechanism of PLB [12–14]. In the "bellflower" structure of PLB pentamers in DPC micelles, the cytoplasmic a-helical domains of PLB are pointing away from the membrane surface [15]. Solid-state NMR studies on AFA-PLB incorporated into 1,2-dimyristoyl-*sn*-glycero-3-phosphocholine (DMPC) lipid bilayers indicate that the cytoplasmic domain exhibits a high degree of structural disorder [16]. Additional solid-state NMR studies of PLB in the presence of Ca^{2+}-ATPase, did not detect the presence of a populated dynamic state of PLB after formation of the PLB/SERCA complex [17].

Structural studies provide a clearer and more complete picture on the working mechanism of PLB, but there are still several unresolved issues, especially the conformation and dynamics of the cytoplasmic domain. It should also be noted that the static three-dimensional PLB structure itself does not immediately make the working mechanism clear. Protein dynamics have been shown to play an integral role in the function of membrane protein systems [19–21].

Abbreviations: CD, circular dichroism; CP-MAS, cross-polarization magic-angle-spinning; PLB, phospholamban; POPC, 1-palmitoyl-2-oleoyl-*sn*-glycero-3-phosphocholine; MLVs, multilamellar vesicles; SR, sarcoplasmic reticulum; SERCA, sarco(endo) plasmic reticulum calcium ATPase

* Corresponding author. Tel.: +1 513 529 3338; fax: +1 513 529 5715.
E-mail address: garylorigan@muohio.edu (G.A. Lorigan).

0005-2736/$ – see front matter © 2009 Elsevier B.V. All rights reserved.
doi:10.1016/j.bbamem.2009.09.025

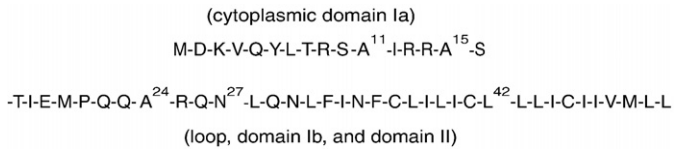

Fig. 1. Amino acid sequence of wild-type phospholamban. The ^{2}H-labeling sites are Ala15, Ala24, and Leu42, and the ^{15}N-labeling sites are Ala11 and Leu42. The four dynamic domains are: Ia (residues 1–16), loop (residues 17–22), Ib (residues 23–30) and II (residues 31–52), following the convention in ref. [12].

The inhibitory effects of PLB involve amino acids in both the transmembrane domain and the cytoplasmic domain. The hinge loop of PLB that connects the two a-helixes has been suggested to regulate a long-range coupling between the cytoplasmic domain and the transmembrane domain and has unique structural and functional implications [22–24]. Specifically, the Asn27 to Ala mutant (N27A-PLB) maintains a normal pentamer to monomer ratio, has been shown to be a superinhibitor of SERCA Ca^{2+} affinity and of cardiac contractility *in vivo*, and to be involved in heart failure [24]. This mutation in the hinge region of PLB was reported to be involved in the structural and functional roles in transmitting PLB's regulatory effects on SERCA [23].

Previously, we have investigated the wild-type PLB as well as its phosphorylated form in lipid membranes with different solid-state NMR spectroscopic techniques [25–30]. In the present study, the effects of the N27A mutation on the side-chain and backbone dynamics of PLB were investigated using solid-state ^{2}H and ^{15}N NMR spectroscopy of site-specifically b-methyl (CD_3) labeled Ala and δ-methyl labeled Leu, or ^{15}N-amide labeled Ala and Leu, located in the three domains of PLB, respectively.

2. Materials and methods

2.1. Materials

All synthetic phospholipids were purchased from Avanti Polar Lipids (Alabaster, AL). The phospholipids were dissolved in chloroform and stored at −20 °C before use. 2,2,2-Trifluoroethanol (TFE), N-[2-hydroxyethyl]piperazine-N′-2-ethane sulfonic acid (HEPES) and acrylamide were obtained from Sigma-Aldrich (St. Louis, MO). Fmoc amino acids and other chemicals for peptide synthesis were purchased from Novabiochem (San Diego, CA). ^{15}N- and ^{2}H- L-Ala N-Fmoc derivative, ^{15}N- and ^{2}H- L-Leu N-Fmoc derivative, $^{15}NH_4Cl$, and deuterium-depleted water were purchased from Isotec™/Sigma-Aldrich (Miamisburg, OH). Precise™ protein pre-cast gels and protein molecular weight markers for sodium dodecyl sulfate polyacrylamide gel electrophoresis (SDS-PAGE) were purchased from Thermo Scientific (Rockford, IL) and Invitrogen (Carlsbad, CA), respectively.

2.2. Peptide synthesis, purification and characterization

The peptides were synthesized with an ABI 433A peptide synthesizer (Applied Biosystems, Foster City, CA) using the Fast-fluorenylmethoxycarbonyl strategy as descried previously [29]. The peptides were purified with an ÄKTA™ purifier HPLC chromatography system (GE Healthcare (Pharmacia) Uppsala, Sweden) equipped with a reverse-phase polymer column. The peptides were lyophilized and then characterized with an Ultraflex™ matrix-assisted laser desorption ionization time-of-flight/time-of-flight (MALDI-TOF/TOF) mass spectrometer (Bruker Daltonics Inc. Billerica, MA).

SDS-PAGE of the synthetic wild-type PLB and N27A-PLB mutant was conducted according to Wegener and Jones [31] using a 4 to 15% acrylamide gradient in the resolving gel. After electrophoresis, the gel was stained for 30 min with Coomassie Blue followed by overnight destaining.

The circular dichroism (CD) spectra of PLB and N27A-PLB were collected in different media including TFE/H_2O (80:20) solvent and 1,2-diheptanoyl-*sn*-glycero-3-phosphocholine (DHPC) micelles with a J-810 circular dichroism spectropolarimeter (JASCO Inc. Easton, MD). The measurements were conducted at 25 °C in a water-jacketed 1 mm cylindrical quartz cuvette (Hellma Int. Inc. Plainview, NY) over the wavelength range 180–300 nm. Each spectrum was the average of eight scans and was corrected for spurious signals generated by the medium. The peptide concentrations were determined by absorbance at 280 nm on a NanoDrop® UV/visible spectrophotometer (NanoDrop, Wilmington, DE).

2.3. Sample preparation

For ^{2}H- and ^{15}N- solid-state NMR experiments, site-specific ^{2}H- or ^{15}N-labeled WT-PLB or N27A-PLB sample were prepared in 1-palmitoyl-2-oleoyl-*sn*-glycero-3-phosphocholine (POPC) as described previously [29]. Approximately 11 mg of the isotope-labeled peptide was first dissolved in a minimal amount of TFE prior to cosolubilizing with 35 mg of the POPC lipids (at a peptide concentration of 4 mol% with respect to lipids). The chloroform and TFE solvents were removed slowly under a steady stream of N_2 gas and the samples were dried overnight in a vacuum desiccator. The resulting mixtures were hydrated with 95 mL HEPES buffer (30 mM HEPES, and 20 mM NaCl, pH 7.0). The hydrated samples underwent through 5–10 freeze–thaw cycles using liquid nitrogen to increase the homogeneity of the vesicles. The pellet (60–80 mg) was transferred to a 4 mm MAS rotor for ^{2}H and ^{15}N NMR spectroscopic studies.

2.4. Solid-state NMR spectroscopy

All NMR experiments were performed on a 500 MHz Bruker Avance wide-bore NMR spectrometer (Bruker BioSpin, Rheinstetten, Germany) using a 4 mm triple resonance CP-MAS probe (Bruker BioSpin).

^{2}H NMR spectra were acquired at a ^{2}H frequency of 76.773 MHz. A quadrupolar echo pulse sequence (90°–τ_1–90°–τ_2–acquire) [32] was used, with a recycle delay of 300 ms, echo delay τ_1 of 40 μs, τ_2 of 35 μs, and ^{2}H 90° of 3.0 μs. The spectral width was set to 100 kHz. 20 K scans were averaged and the free induction delays (FIDs) were processed with a linebroadening of 200 Hz with the Bruker Topspin 2.0 software.

^{15}N NMR spectra were acquired at a ^{15}N frequency of 50.680 MHz using a RAMP cross-polarization pulse sequence with ^{1}H decoupling. A 4.8 ms ^{1}H 90° pulse, 1.5 ms contact time, 500 ppm sweep width, and a 4 s recycle delay were used. 120 K scans were averaged for the static ^{15}N CP NMR experiments at −25 °C and 25 °C respectively. The FIDs were processed with a linebroadening of 300 Hz. ^{15}N NMR spectra were simulated with the DMFIT software program [33].

3. Results and discussion

3.1. SDS-PAGE gel and circular dichroism spectra of wild-type PLB and N27A-PLB

The oligomerization states of the synthetic N27A-PLB mutant as well as the wild-type PLB were investigated with SDS-polyacrylamide gel electrophoresis. As shown in Fig. 2 in the left lane, the band above 22 kDa was suggested to be the pentameric form of wild-type PLB [34]. The SDS-PAGE gel shows that both the wild-type PLB and the N27A-PLB mutant are predominantly in the pentameric states and their migration patterns are very similar to each other. The N27A mutation does not significantly change the oligomerization state of PLB, which is consistent with the previous reports where the PLB N27A mutant exhibits primarily pentameric

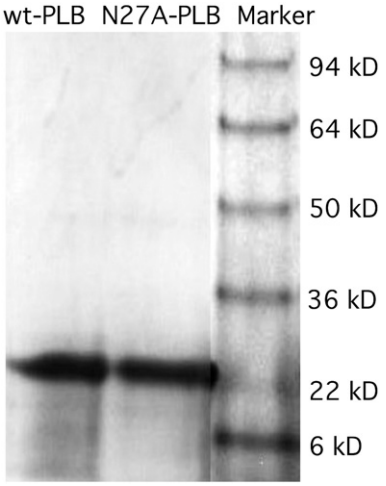

Fig. 2. SDS-PAGE of the synthetic wild-type PLB and N27A-PLB mutant. PLB was loaded on a 4–15% polyacrylamide gradient gel. After electrophoresis, the gel was stained with Coomassie blue followed by overnight destaining.

assembly in native SR membranes [22,24]. When co-expressed with SERCA2a, the monomer percent was calculated to be 10.1% for N27A-PLB, while wild-type PLB exists in 10.9% monomer form [22]. The comparable pentamer:monomer ratios of wild-type PLB and N27A-PLB avoid the potential effects of different oligomerization states on the structural and dynamical properties discussed in this manuscript.

Fig. 3 shows the circular dichroism spectra of both wild-type PLB and the N27A-PLB mutant. The spectra indicate that the proteins are largely a-helical when reconstituted into DHPC micelles as well as in TFE/H_2O solvent, as seen from the characteristic positive signal at 190 nm and two negative ellipticity humps at 207 and 222 nm, which are in well agreement with the previous results [35,36]. CD measurements also provide an estimate of the percentage of a-helix formation. The N27A mutation of PLB decreases the a-helical secondary structure percentage slightly, as indicated by the decreased ellipticity of N27A-PLB when compared with WT-PLB after normalizing the ellipticity against the peptide concentration. The reduced a-helical secondary structure percentage is consistent with a previous report, which showed that the presence of a N27A mutation decreased the helical content of PLB [23].

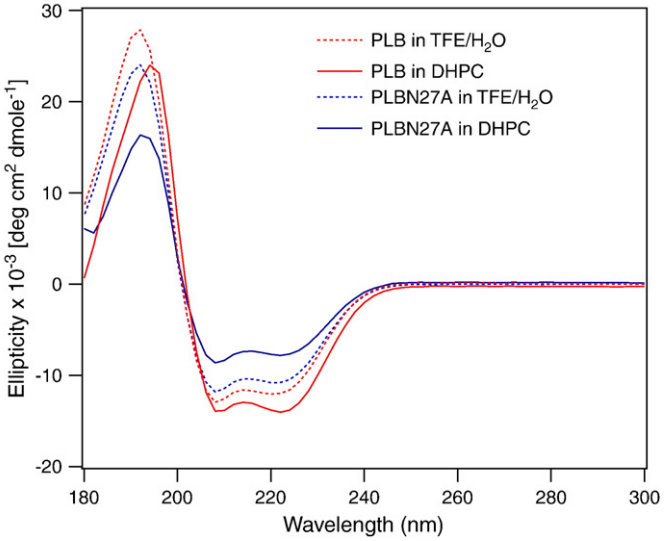

Fig. 3. Circular dichroism spectra of wt-PLB (in red) and the N27A-PLB mutant (in blue) recorded in TFE/H_2O (80:20) (dotted lines) or in DHPC micelles (solid lines) at 25 °C. The spectra, presenting in terms of mean residue ellipticity in [deg cm^2 $domle^{-1}$], were normalized against the peptide concentration after subtracting the contributions from the solvent and lipid vesicles.

3.2. ^{2}H-NMR and side-chain dynamics

Fig. 4 shows the solid-state ^{2}H NMR spectra of site-specific CD_3-labeled N27A-PLB at residues Leu42, Ala24 and Ala15 incorporated into POPC MLVs, along with the corresponding ^{2}H NMR data of wild-type PLB [29]. The three residues are located in the transmembrane domain, linker region, and cytoplasmic domain respectively. The spectra were collected over a temperature range from −25 °C to 50 °C.

The ^{2}H quadrupolar splitting $\Delta\nu_Q$ is defined in Eq. (1) and can be used to describe the motional dynamics of the site-specific CD_3 group labeled peptide reconstituted into randomly dispersed MLVs:

$$\Delta\nu_Q = \frac{3}{8}e^2Q\frac{q}{h}S_{mol}\left(3\cos^2\theta_i - 1\right) \quad (1)$$

where e^2Qq/h is the nuclear quadrupolar coupling constant (165–170 kHz for a C–D bond) [37,38], S_{mol} is the molecular order parameter reflecting orientational fluctuations of the C–D bond relative to the bilayer normal, and θ_i is the average orientation of each C–D bond relative to the bilayer normal.

At −25 °C, the ^{2}H NMR spectra of N27A-PLB with CD_3-labeled at positions Leu42, Ala24 and Ala11 reveal a broad component that is typical of ^{2}H powder pattern spectra having a symmetric Pake doublet. This broad component is from a population of species undergoing slow rotational motions [39,40]. At this temperature, the ^{2}H NMR spectra of all three site-specifically labeled residues of N27A-PLB show similar lineshapes when compared with that of corresponding wild-type PLB residues [29]. However, the ^{2}H NMR spectrum of the CD_3-labeled Ala24 N27A-PLB (Fig. 4B) shows a quadrupolar splitting of about 36.7 kHz, which is slightly reduced from the $\Delta\nu_Q$ value (~40 kHz) of the corresponding wild-type PLB. The decreased splitting suggests that the cytoplasmic domain may be more mobile after the N27A mutation or possibly that the C–D bond could be at a slightly different orientation relative to the bilayer.

At 0 °C, slightly above the POPC's gel-to-lipid-crystalline phase transition temperature (−3 °C), the ^{2}H NMR lineshapes show dramatic differences when comparing the different CD_3-labeling amino acid residue positions. As shown in Fig. 4A, the ^{2}H NMR lineshapes of ^{2}H-Leu42 N27A-PLB reveal a broad component as well as an isotropic component, representing slow motion and rapid motion respectively. This result is very similar to that of wild-type PLB (Fig. 4D).

However, at 0 °C (as shown in Fig. 4B), the ^{2}H NMR spectrum of ^{2}H-Ala24 N27A-PLB reveals an isotropic peak, suggesting that rapid isotropic motion is dominant at this Ala24 position after N27A mutation when compared to the reduced broad component observed in wild-type PLB with CD_3-labeling at the same position (Fig. 4E). This dramatic change in ^{2}H NMR lineshapes indicates that the N27A mutation of PLB leads to more mobile residues at position 24 around the linker region [40].

In Fig. 4C, the ^{2}H NMR spectrum of ^{2}H-Ala15- N27A-PLB also shows a comparable isotropic peak, which is similar with that observed in wild-type PLB with a ^{2}H-label at the same position (Fig. 4F). Both N27A-PLB and wild-type PLB show rapid motion in the cytoplasmic domain as represented by ^{2}H-NMR of ^{2}H-Ala15 PLB.

When the sample temperature was increased to 25 °C and further to 50 °C, slow motion was still observed in the transmembrane domain as revealed by the ^{2}H NMR of ^{2}H-Leu42 N27A-PLB in Fig. 4A. But only rapid isotropic motion can be observed in the linker region

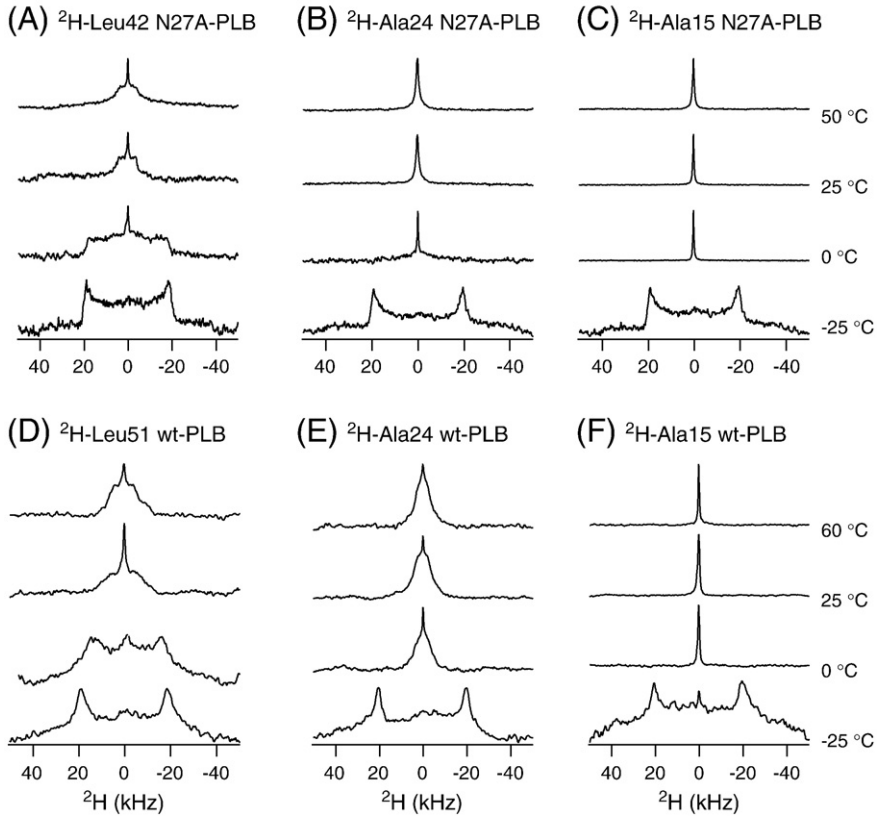

Fig. 4. ^{2}H powder NMR spectra of the N27A-PLB mutant with site-specific CD_3-labels at Leu42 (A) and Ala24 (B), and Ala15 (C) recorded in POPC MLVs at different temperatures. The corresponding ^{2}H NMR spectra of wild-type PLB collected in the same membrane are shown in (D–F) (ref. [29]) for direct comparison.

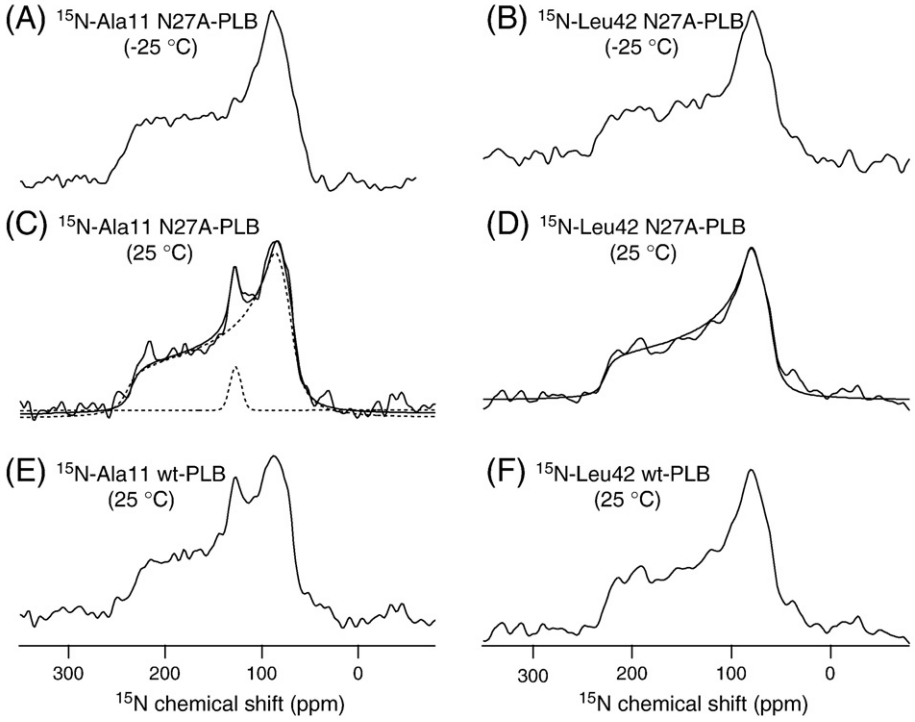

Fig. 5. ^{15}N powder NMR spectra of N27A-PLB with site-specific ^{15}N-labels at Ala11 (A, C) and Leu42 (B, D) reconstituted into POPC MLVs at −25 °C and 25 °C, respectively. The corresponding WT ^{15}N NMR powder spectra are shown in (E) and (F). The smooth simulated spectrum (solid line) in (C) was generated by summation of two CSA components (two dotted lines). The smooth simulated spectrum in (D) was generated using one CSA component.

and cytoplasmic domain at high temperature. The different side-chain dynamic properties of the Ib domain after N27A mutation are clearly visible when comparing Fig. 4B and E.

3.3. ^{15}N-NMR and backbone dynamics

The effect of N27A mutation on the backbone dynamics of PLB was further investigated with ^{15}N NMR of site-specific ^{15}N-labels at Ala11 and Leu42 PLB incorporated into POPC MLVs (Fig. 5A–D), representing the cytoplasmic domain and the transmembrane domain of PLB respectively. The ^{15}N NMR spectra were collected at both −25 and 25 °C. As expected, at both −25 °C and 25 °C, the ^{15}N NMR spectra of ^{15}N-Leu42 N27A-PLB (Fig. 5B and D) reveal powder pattern spectra that are very similar with that of WT-PLB (Fig. 5F), and the simulation of ^{15}N NMR spectrum at 25 °C gave very similar ^{15}N chemical shift tensors (σ_{11} of 56, σ_{22} of 78 and σ_{33} of 228 ppm) and chemical shift anisotropy width (CSA width of 172 ppm) when compared with that of the corresponding ^{15}N-labeled wild-type PLB [29], suggesting that N27A mutation does not induce significant changes in the transmembrane backbone dynamics of PLB. The ^{15}N CSA results are similar to other patterns observed in the literature [40,41]. The ^{15}N NMR spectrum of PLB N27A labeled at Leu42 showed only one broad powder pattern component at 25 °C, indicating that these amide sites are immobile on the ^{15}N NMR time scale in POPC bilayers at room temperature.

However, as shown in Fig. 5C at 25 °C, the ^{15}N NMR spectrum of N27A-PLB with ^{15}N-labeling at Ala11 yields an isotropic component as well as a powder pattern component. This indicates that the cytoplasmic domain of N27A-PLB has two main different conformational populations: one that is immobile and a second component that is dynamically averaged on the ^{15}N NMR time scale. This isotropic component observed for the cytoplasmic domain of Ala11 disappears at −25 °C as shown in Fig. 5A, confirming that the isotropic component observed at 25 °C results from peptide backbone motion.

4. Discussion

The PLB N27A mutant has been shown to function as a superinhibitor of SERCA Ca^{2+} affinity and cardiac contractility *in vivo* [24], and the increased inhibition of Ca^{2+} sequestration may be a causative factor finally leading to heart failure [23]. The subcellular mechanisms of the enhanced inhibitory function of pentameric N27A-PLB mutant are not clear at this time.

As shown in Fig. 2 as well as other previous studies [22,24], the N27A mutation does not change the oligomerization state of wild-type PLB with the pentamer still being the dominant form. The pentameric N27A-PLB mutant provides an interesting system to study the structural and dynamic properties upon comparison with the pentameric WT form of PLB.

Analysis of the CD spectra in Fig. 3 indicates that the a-helical content of PLB decreases slightly upon N27A mutation. This data agrees with solution NMR studies which revealed an alternation in the a-helical configuration between residues Gln22 to Phe35 for the N27A-PLB mutant [23].

It is generally accepted that wild-type PLB consists of an a-helical transmembrane domain connected to a mobile a-helical cytoplasmic domain via a less structurally ordered linker region. The exact starting and ending positions of these three regions proposed in the literature are not consistent and may be dependent on the exact reconstituted environment of membrane-bound PLB [9–11,13,15–16]. A very recent solid-state NMR study indicated that in the presence of SERCA, AFA-PLB has a short N-terminal (Val4–Arg13) and a long C-terminal (Gln29–Val49) helix intersected by a linker of reduced structural order from Arg14 to Gln22, and the C-terminal helix comprised of residues Ala24–Gln26 [17].

PLB regulates intracellular SR Ca^{2+} homeostasis through inhibitory interaction with SR Ca^{2+}-ATPase. The 27 position of PLB is believed to play a crucial role in interacting with Ca^{2+} ATPase [22–24]. The hinge region in PLB may interact directly with the SR Ca^{2+} ATPase [42]. Interaction of domain Ib with Ca^{2+}-ATPase is supported by the enhanced inhibitory capacity of the N27A mutant. In particular, based on chemical cross-linking studies, it has been suggested that an interaction of the PLB transmembrane helix at Asn27 with the cytosolic extension of the transmembrane helix 4 (M4) of SERCA at Leu321 leads to a potential unwinding of the helix [43].

The amino acid sequence of PLB is highly conserved, and although all species contain asparagine (Asn) at residue 27, human PLB is unique in containing a lysine (Lys). Both asparagine and lysine have a carboxamide group and an ε-amino group respectively which often form hydrogen bond interactions with the peptide backbone. Asparagine residues are generally found near the beginning and the end of a-helices. Its role can be thought as “capping” the hydrogen bonding interactions which would otherwise be satisfied by the polypeptide backbone. It has been suggested that this unique amino acid sequence at the 27 position may be critical in maintaining a high cardiac reserve [44].

As expected, the N27A mutation does not induce dramatic dynamic changes in the transmembrane a-helix as monitored with ^{2}H or ^{15}N site-specific labels at position Leu42. However, the N27A mutation increased the side-chain dynamics at Ala24 as revealed from ^{2}H NMR. Because the CD_3 group in Ala is directly connected to the a-carbon, the C–D bonds can undergo isotropic reorientation only if the backbone of the residues undergoes isotropic reorientation owing to the constraints imposed by the side chains [40]. Thus, the dynamic motions observed in the case of the CD_3 group of Ala reflect the dynamics of the backbone. The results suggest increased backbone dynamics at the 24 position upon N27A mutation. The superinhibitory effects resulting from the N27A mutation may involve conformational changes that enhance the association between PLB and SERCA. An enhanced association between PLB and SERCA would be consistent with the inability of phosphorylation, to provide full relief of the superinhibitory effect of the N27A-PLB mutant [24]. This may illustrate again that the structural dynamics of PLB can be “tuned”, either by mutation or by phosphorylation to control its inhibition function on SERCA [45].

PLB, as an inhibitor, decreases the affinity of SERCA for Ca^{2+}. N27A-PLB, functioning as a superinhibitor, decreases the affinity of SERCA for Ca^{2+} even more when compared to the wild-type PLB. The increased mobility of Ala24 in the linker region upon N27A mutation may introduce more conformational flexibility of the hinge region which may be beneficial for the adaption of the cytoplasmic and transmembrane SERCA binding sites. The easier adaption may enhance the association between N27A-PLB and SERCA, thus, resulting in the super inhibitory effect of N27A-PLB.

Acknowledgements

We would like to thank Dr. Thusitha Gunasekera for the help with the SDS-PAGE gels. This work was supported by NIH grants (GM080542 and GM080542Z) and an AHA grant (0755602B). The Bruker 500 MHz wide-bore NMR spectrometer was obtained from an NSF grant (10116333).

References

[1] H.K. Simmerman, L.R. Jones, Phospholamban: protein structure, mechanism of action, and role in cardiac function, Physiol. Rev. 78 (1998) 921–947.
[2] D.H. MacLennan, E.G. Kranias, Phospholamban: a crucial regulator of cardiac contractility, Nat. Rev. Mol. Cell Biol. 4 (2003) 566–577.
[3] A.D. Wegener, H.K. Simmerman, J.P. Lindemann, L.R. Jones, Phospholamban phosphorylation in intact ventricles. Phosphorylation of serine 16 and threonine 17 in response to beta-adrenergic stimulation, J, Biol. Chem. 264 (1989) 11468–11474.

[4] C.B. Karim, J.D. Stamm, J. Karim, L.R. Jones, D.D. Thomas, Cysteine reactivity and oligomeric structure of phospholamban and its mutants, Biochemistry 37 (1998) 12074–12081.
[5] Y. Kimura, K. Kurzydlowski, M. Tada, D.H. MacLennan, Phospholamban inhibitory function is activated by depolymerization, J. Biol. Chem. 272 (1997) 15061–15064.
[6] R.L. Cornea, L.R. Jones, J.M. Autry, D.D. Thomas, Mutation and phosphorylation change the oligomeric structure of phospholamban in lipid bilayers, Biochemistry 36 (1997) 2960–2967.
[7] D.L. Stokes, A.J. Pomfret, W.J. Rice, J.P. Glaves, H.S. Young, Interactions between Ca^{2+}-ATPase and the pentameric form of phospholamban in two-dimensional co-crystals, Biophys. J. 90 (2006) 4213–4223.
[8] A. Ramamoorthy (Ed.), NMR Spectroscopy of Biological Solids, CRC/Taylor and Francis Group, Boca Raton, 2005.
[9] A. McDermott, Structure and dynamics of membrane proteins by magic angle spinning solid-state NMR, Annu. Rev. Biophys. 38 (2009) 385–403.
[10] R.C. Page, C. Li, J. Hu, F.P. Gao, T.A. Cross, Lipid bilayers: an essential environment for the understanding of membrane proteins, Magn. Reson. Chem. 45 (2007) S2–S11.
[11] C.B. Karim, T.L. Kirby, Z.W. Zhang, Y. Nesmelov, D.D. Thomas, Phospholamban structural dynamics in lipid bilayers probed by a spin label rigidly coupled to the peptide backbone, Proc. Natl. Acad. Sci. U.S.A. 101 (2004) 14437–14442.
[12] J. Zamoon, A. Mascioni, D.D. Thomas, G. Veglia, NMR solution structure and topological orientation of monomeric phospholamban in dodecylphosphocholine micelles, Biophys. J 85 (2003) 2589–2598.
[13] N.J. Traaseth, R. Verardi, K.D. Torgersen, C.B. Karim, D.D. Thomas, G. Veglia, Spectroscopic validation of the pentameric structure of phospholamban, Proc. Natl. Acad. Sci. U.S.A. 104 (2007) 14676–14681.
[14] N.J. Traaseth, K.N. Ha, R. Verardi, L. Shi, J.J. Buffy, L.R. Masterson, G. Veglia, Structural and dynamic basis of phospholamban and sarcolipin inhibition of Ca^{2+}-ATPase, Biochemistry 47 (2008) 3–13.
[15] K. Oxenoid, J.J. Chou, The structure of phospholamban pentamer reveals a channel-like architecture in membranes, Proc. Natl. Acad. Sci. U.S.A. 102 (2005) 10870–10875.
[16] O.C. Andronesi, S. Becker, K. Seidel, H. Heise, H.S. Young, M. Baldus, Determination of membrane protein structure and dynamics by magic-angle-spinning solid-state NMR spectroscopy, J. Am. Chem. Soc. 127 (2005) 12965–12974.
[17] K. Seidel, O.C. Andronesi, J. Krebs, C. Griesinger, H.S. Young, S. Becker, M. Baldus, Structural characterization of Ca^{2+}-ATPase-bound phospholamban in lipid bilayers by solid-state nuclear magnetic resonance (NMR) spectroscopy, Biochemistry 47 (2008) 4369–4376.
[18] E. Hughes, J.C. Clayton, D.A. Middleton, Probing the oligomeric state of phospholamban variants in phospholipid bilayers from solid-state NMR measurements of rotational diffusion rates, Biochemistry 44 (2005) 4055–4066.
[19] S.J. Opella, Protein dynamics by solid state nuclear magnetic resonance, Methods Enzymol 131 (1986) 327–361.
[20] A. Krushelnitskya, D. Reichertb, Solid-state NMR and protein dynamics, Prog. Nucl. Magn. Reson. Spectrosc. 47 (2005) 1–25.
[21] M. Hong, Structure, topology, and dynamics of membrane peptides and proteins from solid-state NMR spectroscopy, J. Phys. Chem. B 111 (2007) 10340–10351.
[22] Y. Kimura, M. Asahi, K. Kurzydlowski, M. Tada, D.H. MacLennan, Phospholamban domain Ib mutations influence functional interactions with the Ca^{2+}-ATPase isoform of cardiac sarcoplasmic reticulum, J. Biol. Chem. 273 (1998) 14238–14241.
[23] A.G. Schmidt, J. Zhai, A.N. Carr, M.J. Gerst, J.N. Lorenz, P. Pollesello, A. Annila, B.D. Hoit, E.G. Kranias, Structural and functional implications of the phospholamban hinge domain: impaired SR Ca^{2+} uptake as a primary cause of heart failure, Cardiovasc. Res. 56 (2002) 248–259.
[24] J. Zhai, A.G. Schmidt, B.D. Hoit, Y. Kimura, D.H. MacLennan, E.G. Kranias, Cardiac-specific overexpression of a superinhibitory pentameric phospholamban mutant enhances inhibition of cardiac function *in vivo*, J. Biol. Chem. 275 (2000) 10538–10544.
[25] E.K. Tiburu, E.S. Karp, P.C. Dave, K. Damodaran, G.A. Lorigan, Investigating the dynamic properties of the transmembrane segment of phospholamban incorporated into phospholipid bilayers utilizing ^{2}H and ^{15}N solid-state NMR spectroscopy, Biochemistry 43 (2004) 13899–13909.
[26] E.S. Karp, E.K. Tiburu, S. Abu-Baker, G.A. Lorigan, The structural properties of the transmembrane segment of the integral membrane protein phospholamban utilizing ^{13}C CPMAS, ^{2}H, and REDOR solid-state NMR spectroscopy, Biochim. Biophys. Acta-Biomembranes 1758 (2006) 772–780.
[27] S. Abu-Baker, G.A. Lorigan, Phospholamban and its phosphorylated form interact differently with lipid bilayers: A ^{31}P, ^{2}H, and ^{13}C solid-state NMR spectroscopic study, Biochemistry 45 (2006) 13312–13322.
[28] J.-X. Lu, K. Damodaran, G.A. Lorigan, Probing membrane topology by high-resolution ^{1}H-^{13}C heteronuclear dipolar solid-state NMR spectroscopy, J. Magn. Reson. 178 (2006) 283–287.
[29] S. Abu-Baker, J.-X. Lu, S. Chu, C.C. Brinn, C.A. Makaroff, G.A. Lorigan, Side-chain and backbone dynamics of phospholamban in phospholipid bilayers utilizing ^{2}H and ^{15}N solid-state NMR spectroscopy, Biochemistry 46 (2007) 11695–11706.
[30] S. Abu-baker, J.-X. Lu, S. Chu, K.K. Shetty, P.L. Gor'kov, G.A. Lorigan, The structural topology of wild-type phospholamban in oriented lipid bilayers using ^{15}N solid-state NMR spectroscopy, Protein Sci 16 (2007) 2345–2349.
[31] A.D. Wegener, L.R. Jones, Phosphorylation-induced mobility shift in phospholamban in sodium dodecyl sulfate-polyacrylamide gels. Evidence for a protein structure consisting of multiple identical phosphorylatable subunits, J. Biol. Chem. 259 (1984) 1834–1841.
[32] J.H. Davis, K.R. Jeffrey, M. Bloom, M.I. Valic, T.P. Higgs, Quadrupole echo deuteron magnetic resonance spectroscopy in ordered hydrocarbon chains, Chem. Phys. Lett. 42 (1976) 390–394.
[33] D. Massiot, F. Fayon, M. Capron, I. King, S. Le Calvé, B. Alonso, J.-O. Durand, B. Bujoli, Z. Gan, G. Hoatson, Modelling one- and two-dimensional solid-state NMR spectra, Magn. Reson. Chem. 40 (2002) 70–76.
[34] M. Tada, M.A. Kirchberger, A.M. Katz, Phosphorylation of a 22,000-dalton component of the cardiac sarcoplasmic reticulum by adenosine 3′:5′-monophosphate-dependent protein kinase, J. Biol. Chem. 250 (1975) 2640–2647.
[35] T. Vorherr, A. Wrzosek, M. Chiesi, E. Carafoli, Total synthesis and functional properties of the membrane-intrinsic protein phospholamban, Protein Sci 2 (1993) 339–347.
[36] I.T. Arkin, M. Rothman, C.F.C. Ludlam, S. Aimoto, D.M. Engelman, K.J. Rothschild, S. O. Smith, Structural model of the phospholamban ion channel complex in phospholipid membranes, J. Mol. Biol. 248 (1995) 824–834.
[37] J. Seelig, Deuterium magnetic resonance: theory and applications to lipid membranes, Q. Rev. Biophys. 10 (1977) 353–418.
[38] J.H. Davis, The description of membrane lipid conformation, order and dynamics by ^{2}H-NMR, Biochim. Biophys. Acta 737 (1983) 117–171.
[39] J.C. Clayton, E. Hughes, D.A. Middleton, Spectroscopic studies of phospholamban variants in phospholipid bilayers, Biochem. Soc. Trans. 33 (2005) 913–915.
[40] L.A. Colnago, K.G. Valentine, S.J. Opella, Dynamics of fd coat protein in the bacteriophage, Biochemistry 26 (1987) 847–854.
[41] S. Kim, T.A. Cross, Uniformity, ideality, and hydrogen bonds in transmembrane alpha-helices, Biophys J 83 (2002) 2084–2095.
[42] C. Toyoshima, M. Asahi, Y. Sugita, R. Khanna, T. Tsuda, D.H. MacLennan, Modeling of the inhibitory interaction of phospholamban with the Ca^{2+} ATPase, Proc. Natl. Acad. Sci. U.S.A. 100 (2003) 467–472.
[43] T. Morita, D. Hussain, M. Asahi, T. Tsuda, K. Kurzydlowski, C. Toyoshima, D.H. Maclennan, Interaction sites among phospholamban, sarcolipin, and the sarco (endo)plasmic reticulum Ca^{2+}-ATPase, Biochem. Biophys. Res. Commun. 369 (2008) 188–194.
[44] W. Zhao, Q. Yuan, J. Qian, J.R. Waggoner, A. Pathak, G. Chu, B. Mitton, X. Sun, J. Jin, J.C. Braz, H.S. Hahn, Y. Marreez, F. Syed, P. Pollesello, A. Annila, H.S. Wang, J.J. Schultz, J.D. Molkentin, S.B. Liggett, G.W. Dorn, E.G. Kranias, The presence of Lys27 instead of Asn27 in human phospholamban promotes sarcoplasmic reticulum Ca^{2+}-ATPase superinhibition and cardiac remodeling, Circulation 113 (2006) 995–1004.
[45] K.N. Ha, N.J. Traaseth, R. Verardi, J. Zamoon, A. Cembran, C.B. Karim, D.D. Thomas, G. Veglia, Controlling the inhibition of the sarcoplasmic Ca^{2+}-ATPase by tuning phospholamban structural dynamics, J. Biol. Chem. 282 (2007) 37205–37214.